JOURNAL OF THE AMERICAN CHEMICAL SOCIETY

Article

pubs.acs.org/JACS

Improved Quenched Fluorescent Probe for Imaging of Cysteine Cathepsin Activity

Martijn Verdoes,[*,†,∥] Kristina Oresic Bender,[†] Ehud Segal,[†] Wouter A. van der Linden,[†] Salahuddin Syed,[†] Nimali P. Withana,[†] Laura E. Sanman,[†,‡] and Matthew Bogyo[*,†,‡,§]

Departments of [†]Pathology, [‡]Cancer Biology Program, and [§]Microbiology and Immunology, Stanford School of Medicine, 300 Pasteur Drive, Stanford, California 94305-5324, United States

Supporting Information

ABSTRACT: The cysteine cathepsins are a family of proteases that play important roles in both normal cellular physiology and many human diseases. In cancer, the activity of many of the cysteine cathepsins is upregulated and can be exploited for tumor imaging. Here we present the design and synthesis of a new class of quenched fluorescent activity-based probes (qABPs) containing a phenoxymethyl ketone (PMK) electrophile. These reagents show enhanced in vivo properties and broad reactivity resulting in dramatically improved labeling and tumor imaging properties compared to those of previously reported ABPs.

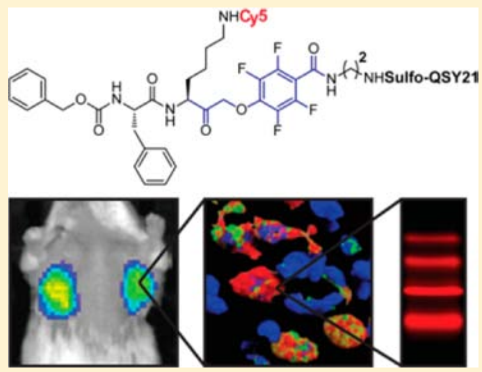

INTRODUCTION

The cysteine cathepsins are a family of proteases that play important roles in health and disease.[1] Although their function has mainly been described as being confined to the endosomal pathway, evidence is accumulating that they are major regulators of matrix degradation and cell motility, suggesting that they also function in an extracellular context.[2] Members of the cysteine cathepsin family have also been shown to be major players in the development and progression of several types of cancer.[3,4] Furthermore, changes in the expression of the endogenous inhibitors of the cathepsins, the cystatins, take place during cancer progression.[5] These observations, in combination with the dynamic nature of the intracellular and extracellular milieus, stress the importance of tools that allow the direct assessment of the activity of these proteases in the context of a native tumor microenvironment. Activity-based probes (ABPs) are small-molecule tools that allow the dynamic monitoring of protease activity. These reagents form activity-dependent covalent bonds with protease active site nucleophiles, thereby providing a readout of the levels of active protease in a cell, tissue, or even whole organism.[6] Several classes of ABPs targeting the cysteine cathepsin family have been reported previously.[7] In particular, fluorescently quenched ABPs (qABPs) have proven to be powerful tools for the noninvasive optical imaging of cancer and subsequent characterization of the target cathepsins on a histological, cellular, and protein level.[8,9]

In this work, we set out to develop a qABP with overall improved in vivo tumor imaging properties compared to those of existing qABPs. We therefore decided to optimize three major elements of the probe: the quencher, the linker, and the electrophilic "warhead". One of the biggest drawbacks of the cysteine cathepsin qABPs reported to date is their relatively poor aqueous solubility. Therefore, we introduced sulfonate groups into the QSY21 quencher[10] in order to improve the water solubility and thereby the biodistribution of the probe. We also varied the length of the spacer tethering the electrophile and the quencher in order to decrease the lipophilicity of the qABP. Finally, we explored a new electrophile in order to increase the range of possible cathepsin targets. Because several members of the cysteine cathepsin family are upregulated in a variety of cancers, mainly but not exclusively as a result of the infiltration of immune cells with high cysteine cathepsin expression,[3] we expected a brighter fluorescence signal in tumors as a result of probes that target a broad spectrum of cysteine cathepsin activities. To obtain a more pan-reactive probe, we aimed to decrease the size and increase the reactivity of the electrophile. All qABPs reported to date are based on the acyloxymethyl ketone (AOMK) electrophile,[8,9,11] with the 2,6-dimethylbenzoic acid-derived AOMK being the most optimal in vivo. This is attributed to the steric protection of the ester bond from cleavage by esterases in the serum. We have previously shown that inhibitors armed with a 2,3,5,6-tetrafluoro-substituted phenoxymethyl ketone (PMK) electrophile had a greater reactivity with cysteine dipeptidyl aminopeptidases compared to their 2,6-dimethylbenzoic acid-derived AOMK counterparts.[12] The introduction of an additional electron-withdrawing amide functionality at the para position of the 2,3,5,6-tetrafluoro PMK to form the tether

Received: June 4, 2013
Published: August 23, 2013

   dx.doi.org/10.1021/ja4056068 | J. Am. Chem. Soc. 2013, 135, 14726−14730

between the electrophile and the quencher would further increase the reactivity of the warhead. The smaller size of the PMK relative to that of the previously reported 2,6-dimethylbenzoic acid-derived AOMKs could also increase the pan-reactivity because the binding grooves of some of the cysteine cathepsins are sterically restricted.[8,13,14] Furthermore, we expect the phenol ether to be more stable in vivo compared to the AOMK electrophile, which contains an ester linkage that can be degraded by esterases.

■ RESULTS AND DISCUSSION

Probe Synthesis. As a starting point for this study, we synthesized seven analogs (**2**−**8**) of the previously reported qABP GB137 (**1**)[8] (Figure 1a). These compounds represent all combinations of the two electrophiles (AOMK and PMK), two quenchers (QSY21 and sulfo-QSY21), and two linker lengths (hexyl and ethyl). The AOMK probes were synthesized using an optimized, solution-chemistry-based procedure as described in the Supporting Information (Scheme S1). The PMK probe synthesis commenced with the commercially available 2,3,5,6-tetrafluoro-4-hydroxybenzoic acid (**9**). The synthesis of qABP **8** is depicted in Scheme 1. After the condensation of monotrityl

Scheme 1. Synthesis of PMK qABP 8

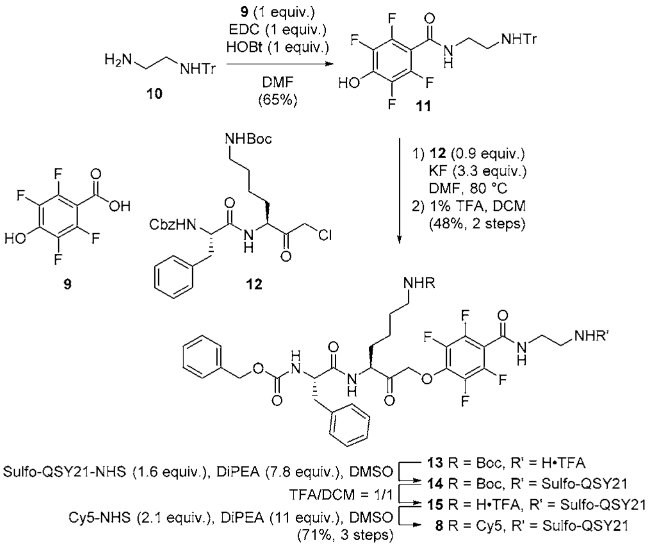

ethylenediamine (**10**), phenol **11** was reacted with chloromethyl ketone **12**[13] at 80 °C under the influence of potassium fluoride in DMF. Heating proved necessary to substitute the chloride with the very deactivated phenolate because no reaction could be observed at room temperature. Subsequent mild acidic cleavage of the trityl protecting group enabled the coupling of water-soluble quencher sulfo-QSY21 to give intermediate **14**. After the acidic removal of the Boc protecting group, the Cy5 dye could be introduced to give PMK qABP **8** in good overall yield.

In Vitro Comparison of qABPs 1−8. We initially tested the specificity and potency of the probes by labeling intact RAW 264.7 cells (mouse leukemic monocyte macrophage cell line) (Figure 1b). We observed several trends in the properties of the probes. All of the sulfo-QSY21-functionalized qABPs (**2**, **4**, **6**, and **8**) showed stronger overall cathepsin labeling compared to that of the more hydrophobic QSY21 containing probes (**1**, **3**, **5**, and **7**). Interestingly, the change in the spacer length from a hexyl to an ethyl linker did not have a dramatic influence on the labeling profile. Perhaps the most striking observation was that the qABPs with the PMK electrophile showed a broader cysteine cathepsin labeling profile than did their AOMK counterparts. Probes **5**−**8** showed robust cathepsin X labeling. Moreover, sulfo-QSY21-functionalized PMK probes **6** and **8** were able to label a higher-molecular-weight pro-form of cathepsin L. The identities of the fluorescently labeled cathepsins were determined by immunoprecipitation (Figure S1a). Upon performing titration labeling experiments in live RAW cells, we observed several other interesting trends. The most hydrophobic qABPs (**1**, **3**, **5**, and **7**) showed only low-level labeling that reached a maximum intensity at 0.5−1 μM (Figures 1c,d and S1b,c), suggesting that their reduced water solubility results in the precipitation of the probes at the higher concentrations. It also became apparent that the shorter spacer length seems to be beneficial, with all probes carrying the ethyl spacer producing brighter labeling signals at 5 μM compared to those of their hexyl-containing counterparts. When comparing the AOMKs and the PMKs, a

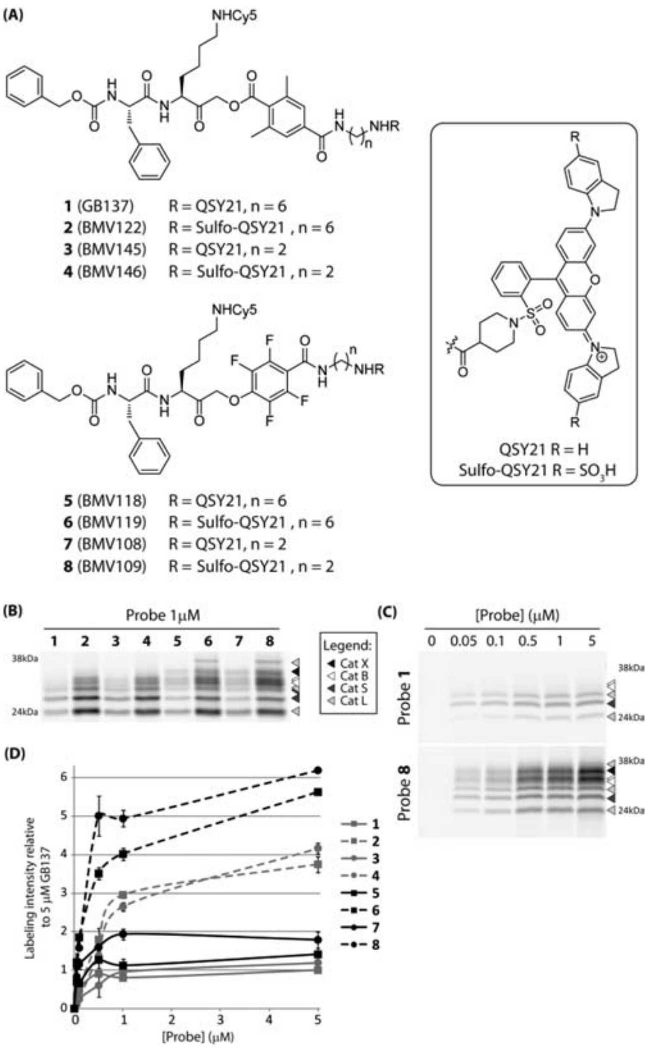

Figure 1. (A) Structures of the qABPs based on GB137 containing the AOMK group (**1**−**4**) and the new probes containing the PMK group (**5**−**8**). (B) Labeling profile of probes **1**−**8** in intact, live RAW cells at 1 μM. (C) Concentration-dependent labeling by probes **1** and **8** in live RAW cells. (D) Total cathepsin labeling intensity of probes **1**−**8** in live RAW cells relative to 5 μM GB137 (**1**).

clear difference in selectivity was observed. The AOMK qABPs preferentially labeled cathepsins S and L and only at higher concentrations labeled cathepsin B. Surprisingly, AOMK qABPs **2**–**4** seem to be capable of labeling cathepsin X even though prior studies showed that several other related AOMKs are incapable of labeling this target (Figure S1b).[14] The PMK qABPs labeled all target cysteine cathepsins with equal intensity, even at the lower probe concentrations, suggesting that they are more sensitive than their AOMK counterparts. Together, these experiments suggest that increased hydrophilicity improves the labeling intensity and that the novel PMK qABPs have a broader, more pan-cysteine cathepsin reactivity.

Further in Vitro Characterization of qABP 8. Because PMK qABP **8** was the most optimal in terms of labeling intensity and broad cathepsin reactivity, we decided to proceed with this probe for further characterization studies. To define target selectivity further, we labeled RAW cell lysates with increasing concentrations of qABP **8** at pH 5.5. These results indicated that the probe has similar potency toward the targeted cysteine cathepsins (B, S, L, and X) with labeling observed at concentrations as low as 5 nM. The labeling of all of the targets was saturated by the 500 nM probe (Figure 2a).

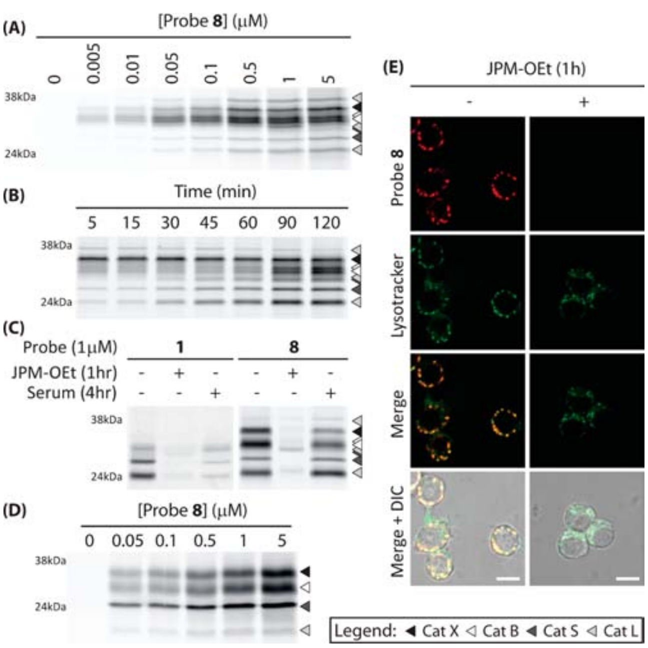

Figure 2. (A) Concentration-dependent labeling of RAW cell lysates by probe **8** at pH 5.5. (B) Labeling time course of 0.5 μM probe **8** in intact, live RAW cells. (C) Inhibition of labeling of probes **1** and **8** in living RAW cells by pretreatment with JPM-OEt (50 μM) and serum stability. (D) Labeling profile of probe **8** in living primary human monocyte-derived macrophages. (E) Live cell fluorescence microscopy of RAW cells exposed to 1 μM probe **8** (red) and lysotracker (green, scale bar 10 μm).

When the probe was used for a time course labeling of live RAW cells at the set concentration of 500 nM, we observed rapid saturation of cathepsin X followed by more slow labeling of cathepsin S, L, and B, with the cathepsin B labeling signal increasing even up to 120 min (Figure 2b). These data suggest that the probe is likely able to access pools of cathepsin X most rapidly, perhaps because of its localization within or on the surface of the cells. It also suggests that cathepsins B and X may be in alternate locations in the cells, which can be accessed by the probe to different extents. When a similar time course labeling experiment of live RAW cells was performed at a probe concentration of 1 μM, a labeling intensity close to saturation was reached as fast as 5 min after exposure to the probe (Figure S1d). This indicates that probe **8** shows very fast cell internalization and labeling kinetics. To test the serum stability of the new PMK probe, we examined the effects of serum exposure on labeling in RAW cells (Figure 2c). Whereas 4 h of serum pre-exposure to original AOMK probe **1** resulted in a loss of nearly 70% of the target labeling, more than 80% of the labeling was retained for PMK qABP **8**. This may be due to the enhanced stability of the PMK over the AOMK toward esterases in the serum. Pretreatment of the cells with cysteine cathepsin inhibitor JPM-OEt blocked more than 90% of this labeling. The exposure of primary human monocyte-derived macrophages to probe **8** revealed that the pan-reactivity of the PMK qABPs was retained for the human enzymes (Figure 2d). Given the improved labeling properties of the PMK probe, we next performed live cell fluorescence microscopy studies. These results confirmed that the probe produced bright, specific labeling signals and that the majority of the probe-labeled cathepsins resides in lysosomes (Figure 2e).

Noninvasive Optical Imaging of Syngeneic Orthotopic Mouse Breast Tumors. Given the positive live cell labeling properties of the new PMK electrophile, we tested best-performing qABP's **2**, **6**, and **8** in a syngeneic orthotopic mouse model of breast cancer.[15] In addition, we compared these probes to original AOMK probe **1** (Figures 3 and S2). 4T1 cells were implanted in the number 2 and 7 mammary fat pads of Balb/c mice, and tumor growth was monitored. When tumors were established, the mice were injected with equimolar amounts of the qABPs (20 nmol) via the tail vein, and the Cy5 fluorescence was noninvasively imaged over time (Figure 3a,b). Again, these results confirmed that qABP **8** proved to be superior. Robust tumor-specific activation of fluorescence with high overall intensity could be observed for probe **8** specifically in the tumor region. Contrary to probe **1**, as soon as 1 h after the injection of probe **8**, tumor margins were already visible with substantial contrast (Figures 2a and S2c), and signals continued to increase up to the end of the time course. Ultimately, probe **8** achieved a more than 20-fold enhanced tumor-specific fluorescence signal compared to that for probe **1**. A good tumor-specific signal was also observed for probe **6** and to a lesser extent for probe **2**, although both still outcompeted the original AOMK probe by more than 10-fold (Figure S2a,b). After the completion of the time course, the tumors were excised and tumor fluorescence was measured ex vivo, followed by homogenization and analysis of the fluorescently labeled proteins by SDS-PAGE (Figures 3c and S2d). The quantification of the ex vivo fluorescence and the total cysteine cathepsin labeling showed a similar trend to that seen in the noninvasive optical imaging studies (Figures 3d and S2e). The labeling profile confirmed that the PMK qABPs are pan-reactive cysteine cathepsin probes in vivo, targeting cathepsins X, B, S, and L with similar labeling intensities, contributing to overall brighter tumor fluorescence. We have previously shown that cathepsin S-directed qABP BMV083 mainly targets M2-type tumor-associated macrophages in 4T1 syngeneic orthotopic mouse breast tumors.[9] To determine the cellular source of probe **8** fluorescence, we performed immunofluorescence staining on tumor tissue sections from probe-labeled mice using macrophage marker CD68 (Figures 3e and S2f). Cy5

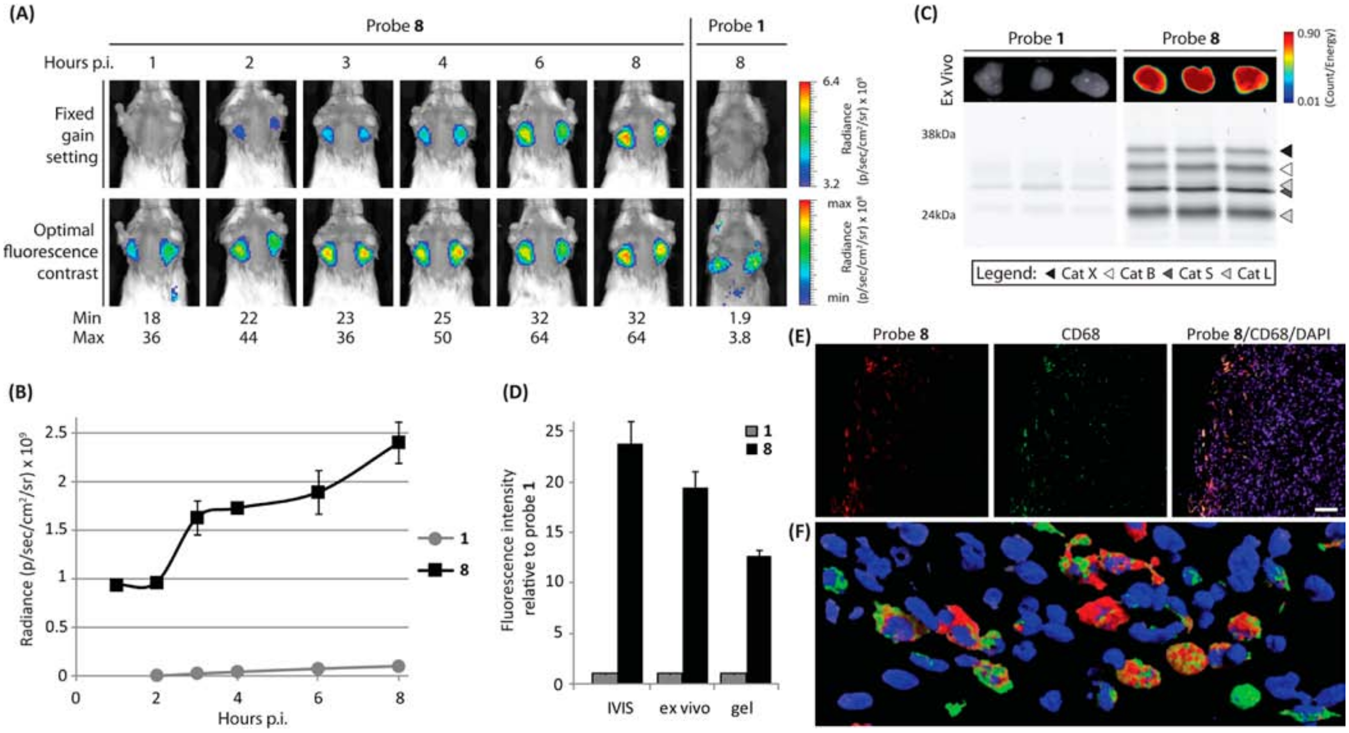

Figure 3. (A) Noninvasive optical imaging time course of tumor-bearing mice injected with probes **8** and **1** (right panels). The lower panels represent the optimal fluorescence contrast at each time point. (B) Time-dependent tumor-specific fluorescence (tumor background) for mice treated with probe **1** or **8** (n = 3; data represent mean values ± standard errors). (C) Ex vivo tumor fluorescence (top panel) and in vivo fluorescently labeled proteins after SDS-PAGE visualized by in-gel fluorescence scanning (lower panel). (D) Fluorescence intensity at the end point of the noninvasive optical imaging study (shown in A). Ex vivo tumor imaging and in-gel fluorescence labeling (shown in C). Intensity relative to probe **1** is depicted (n = 3, data represent mean values ± standard errors). (E) Fluorescence microscopy of probe **8** (red)-treated tumor tissue section with CD68 immunostaining (green) and nuclear staining (DAPI, blue, scale bar 50 μm). (F) Three-dimensional reconstruction of the CLSM of a probe **8** (red)-treated tumor tissue section with CD68 immunostaining (green) and nuclear staining (DAPI, blue).

fluorescence was localized to CD68 positive cells; however, not all CD68 positive cells were probe **8** positive, suggesting different activation states of the tumor-associated macrophages. Probe **8** proves to be able to demarcate the cancer region because of the localization of the probe positive macrophages in the invasive edge of the tumor. More detailed analysis with confocal laser scanning microscopy (CLSM) confirmed that all cells that were positive for probe **8** were CD68 positive (Figure 3f). Taken together, these data confirm that increasing the hydrophilicity of the quencher, shortening the spacer, and introducing a more reactive and sterically less restricted nucleophilic trap resulted in a qABP with a broad cysteine cathepsin reactivity and overall improved in vivo properties.

■ CONCLUSIONS

We have synthesized a novel class of quenched fluorescent activity-based probes bearing a PMK electrophile with greater reactivity and broader selectivity compared to those of previously reported AOMK-based probes. We have furthermore increased the hydrophilicity of qABP by introducing a sulfonated quencher and shortening the spacer tethering between the electrophile and the quencher. This results in greater aqueous solubility and improved in vivo properties, resulting in enhanced specific signal intensity in the noninvasive optical imaging of cancer. Although very distinct functions have been described for some of the cysteine cathepsin family members,[16] other roles are redundant and alterations in the activity of one cathepsin can influence the activity of others. For example, the loss of cathepsin B is compensated for by the increased activity of cathepsin X,[17] and the upregulation of cathepsin B results in the downregulation of cathepsin L.[18] Therefore, a broad spectrum probe is very valuable because it facilitates the readout of multiple cysteine cathepsins in one experiment and enables the comparison of the activities of the individual cathepsins with respect to one another. Furthermore, the overall broad reactivity of the probe within the cathepsin family may facilitate diagnostic applications under a wider range of conditions in which cathepsins are known to be key players. In support of this, the usefulness of pan-reactive ABPs has already been demonstrated by the pan-serine hydrolase fluorophosphonate probes[19] and pan-reactive proteasome probe MV151.[20] The findings that led to the pan-reactive cysteine cathepsin qABP could aid the development of selective chemical tools to study the cathepsin family. Because the PMK-based qABPs are very reactive toward cathepsin X, these scaffolds can be used to generate selective qABPs against this still poorly understood cysteine cathepsin.[14] The optimization of the qABPs presented in this work is an important step toward the potential clinical translation of these contrast agents. Probe **8** proved to be capable of demarcating tumor margins with substantial contrast as soon as 1 h after administration. This finding has particular value for applications in fluorescence-guided cancer surgery,[21] where signal contrast needs to be generated soon after the administration of the contrast agent. In addition, the topical application of a contrast agent capable of distinguishing the tumor margins would allow further flexibility and utility for contrast agents in tumor surgery. We have previously shown that GB119, an AOMK-based qABP, could be applied topically to aid the resection of tumor tissue during cancer surgery.[22] The pan-reactivity that resulted in an enhanced fluorescence signal and the ability of probe **8** to penetrate cells and rapidly saturate the labeling of target cathepsins is tailored for a topically applicable contrast agent. Combined, these enhanced properties of the PMK-containing probes make them important new tools to be added to the current tool box of optical contrast agents. We are currently working toward the preclinical evaluation (i.e., toxicity and GMP production) and testing in human tissues that will be required to initiate clinical studies of the agents in the near future.

■ ASSOCIATED CONTENT

Ⓢ Supporting Information

Experimental details of the synthesis of probes **1**−**8** and biological experiments. Cathepsin target identification by immunoprecipitation. All gels. In vivo data for probe **1**, **2**, and **6**. Control images for microscopy. This material is available free of charge via the Internet at http://pubs.acs.org.

■ AUTHOR INFORMATION

Corresponding Authors

mbogyo@stanford.edu
m.verdoes@ncmls.ru.nl

Present Address

[‖]Department of Tumor Immunology, Nijmegen Centre for Molecular Life Sciences, Radboud University, Nijmegen Medical Centre, Geert Grooteplein 26/28, 6525 GA Nijmegen, The Netherlands.

Notes

The authors declare no competing financial interest.

■ ACKNOWLEDGMENTS

This work was supported by NIH grants R01 EB005011 R01 HL116307 (to M.B.) and The Netherlands Organization for Scientific Research (NWO) Rubicon fellowship (to M.V. and W.A.v.d.L.), and NIH Re-entry into Biomedical Sciences Supplement 3R01EB005011-06S1 (to K.O.B). We thank the members of the Bogyo laboratory for insightful discussions, T. Doyle at the Stanford Small Animal Facility, S. Lynch at the Stanford NMR Facility, and A. Chien and T. McLaughlin at the Stanford Mass Spectrometry Facility for their technical assistance. We also thank Yaron Carmi for assistance with CLSM.

■ REFERENCES

(1) Reiser, J.; Adair, B.; Reinheckel, T. *J. Clin. Invest.* **2010**, *120*, 3421−3431.

(2) Brömme, D.; Wilson, S. Role of Cysteine Cathepsins in Extracellular Proteolysis. In *Biology of Extracellular Matrix*; Parks, W. C., Mecham, R. P., Eds.; Springer: Berlin, 2011; Vol. 2, pp 23−51.

(3) Mohamed, M. M.; Sloane, B. F. *Nat. Rev. Cancer* **2006**, *6*, 764−775.

(4) Palermo, C.; Joyce, J. A. *Trends Pharmacol. Sci.* **2008**, *29*, 22−28.

(5) Cox, J. L. *Front. Biosci.* **2009**, *14*, 463−474.

(6) Serim, S.; Haedke, U.; Verhelst, S. H. *ChemMedChem* **2012**, *7*, 1146−1159.

(7) Edgington, L. E.; Verdoes, M.; Bogyo, M. *Curr. Opin. Chem. Biol.* **2011**, *15*, 798−805.

(8) Blum, G.; von Degenfeld, G.; Merchant, M. J.; Blau, H. M.; Bogyo, M. *Nat. Chem. Biol.* **2007**, *3*, 668−677.

(9) Verdoes, M.; Edgington, L. E.; Scheeren, F. A.; Leyva, M.; Blum, G.; Weiskopf, K.; Bachmann, M. H.; Ellman, J. A.; Bogyo, M. *Chem. Biol.* **2012**, *19*, 619−628.

(10) Xing, B.; Khanamiryan, A.; Rao, J. *J. Am. Chem. Soc.* **2005**, *127*, 4158−4159.

(11) Edgington, L. E.; Verdoes, M.; Ortega, A.; Withana, N. P.; Lee, J.; Syed, S.; Bachmann, M. H.; Blum, G.; Bogyo, M. *J. Am. Chem. Soc.* **2013**, *135*, 174.

(12) Deu, E.; Leyva, M. J.; Albrow, V. E.; Rice, M. J.; Ellman, J. A.; Bogyo, M. *Chem. Biol.* **2010**, *17*, 808−819.

(13) Blum, G.; Mullins, S. R.; Keren, K.; Fonovic, M.; Jedeszko, C.; Rice, M. J.; Sloane, B. F.; Bogyo, M. *Nat. Chem. Biol.* **2005**, *1*, 203−209.

(14) Paulick, M. G.; Bogyo, M. *ACS Chem. Biol.* **2011**, *6*, 563−572.

(15) Lelekakis, M.; Moseley, J. M.; Martin, T. J.; Hards, D.; Williams, E.; Ho, P.; Lowen, D.; Javni, J.; Miller, F. R.; Slavin, J.; Anderson, R. L. *Clin. Exp. Metastasis* **1999**, *17*, 163−170.

(16) Conus, S.; Simon, H. U. *Swiss Med. Wkly.* **2010**, *140*, w13042.

(17) Sevenich, L.; Schurigt, U.; Sachse, K.; Gajda, M.; Werner, F.; Müller, S.; Vasiljeva, O.; Schwinde, A.; Klemm, N.; Deussing, J.; Peters, C.; Reinheckel, T. *Proc. Natl. Acad. Sci. U.S.A.* **2010**, *107*, 2497−2502.

(18) Gopinathan, A.; Denicola, G. M.; Frese, K. K.; Cook, N.; Karreth, F. A.; Mayerle, J.; Lerch, M. M.; Reinheckel, T.; Tuveson, D. A. *Gut* **2012**, *61*, 877.

(19) Liu, Y.; Patricelli, M. P.; Cravatt, B. F. *Proc. Natl. Acad. Sci. U.S.A.* **1999**, *96*, 14694.

(20) Verdoes, M.; Florea, B. I.; Menendez-Benito, V.; Maynard, C. J.; Witte, M. D.; van der Linden, W. A.; van den Nieuwendijk, A. M.; Hofmann, T.; Berkers, C. R.; van Leeuwen, F. W.; Groothuis, T. A.; Leeuwenburgh, M. A.; Ovaa, H.; Neefjes, J. J.; Filippov, D. V.; van der Marel, G. A.; Dantuma, N. P.; Overkleeft, H. S. *Chem. Biol.* **2006**, *13*, 1217.

(21) Keereweer, S.; Hutteman, M.; Kerrebijn, J. D.; van de Velde, C. J.; Vahrmeijer, A. L.; Löwik, C. W. *Curr. Pharm. Biotechnol.* **2012**, *13*, 498.

(22) Cutter, J. L.; Cohen, N. T.; Wang, J.; Sloan, A. E.; Cohen, A. R.; Panneerselvam, A.; Schluchter, M.; Blum, G.; Bogyo, M.; Basilion, J. P. *PLoS One* **2012**, *7*, e33060.